# Practical State Estimation With Event-Triggered Sliding Mode Observer

Saikat Mondal and Abhisek K. Behera, *Member, IEEE*

***Abstract*— This paper deals with the practical state estimation for an uncertain dynamical system under feedback constraints. We propose an event-triggered sliding mode observer to estimate the states in the practical sense, i.e., arbitrary steady-state bound can be achieved for the estimation error irrespective of the disturbance signal. A new sliding mode observer is proposed with the discontinuous output error injection vector of the same order as that of the disturbance vector; therefore the observer can be represented by an interconnection of continuous and discontinuous dynamics. Two scenarios are considered for implementing this observer in the event-triggering framework viz., the actuator side implementation and the sensor side implementation, in which the observer is run at the actuator and sensor sides, respectively. However, the event-triggering mechanism in both cases is placed in the sensor end to regulate the transmission of output/estimated values. It is shown under the observability assumption that the event-triggered observer estimates the states practically with intermittent communication and disturbance input. Finally, we take a practical example to illustrate the state estimation using the proposed sliding mode observer.**

***Index Terms*— Event-based estimation, practical state estimation, robust sliding mode observer.**

## I. Introduction

State estimation is the process of estimating the states of a physical plant using its output information. Traditionally, a dynamical system, known as the observer, is constructed under some suitable assumptions to estimate the states. Although the states are estimated accurately in the ideal case, the performance of these observers is affected under the constraints ( [1], [2]). For instance, in modern applications, the constraints, such as communication burden and energy consumption, have become critical factors in the observer design. In our paper, we address the estimation problem under these constraints in the framework of a popular need-based feedback policy, viz., event-triggering ( [3]).

Event-based sampling strategies have shown a very promising outcome in the controller design for resource-constrained systems ( [3]). Here, the continuous feedback channel is replaced with event-based feedback for scheduling the information exchange online. In fact, the pioneering work of [4] showed that the event (Lebesgue) sampling-based controller achieved superior performance for the (first-order) system than that of the periodic (Reimann) sampling-based controller. Later, this led to the significant development of the event-triggered controller; see [3], [5]–[9] and references cited therein. The analogous problem in state estimation has also been studied for various systems. The event-triggered high-gain observer can estimate the states, but online tuning of parameters becomes difficult because of the dependency on the high-gain parameter ( [10]). Also, the event-based stochastic estimators may not be readily applicable to many nonlinear systems ( [11], [12]). The output feedback stabilization problem was addressed using the event-triggered observers ( [13], [14]). Compared to these observers, sliding mode observers have the advantage of robust state estimation in the presence of disturbances ( [15], [16]). Recently, in [17], the sliding mode observer is applied to detect the denial-of-service attack in a network-based control application. Unfortunately, the study of these observers with feedback constraints is not found in the literature (except in [18]).

S. Mondal and A. K. Behera are with the Department of Electrical Engineering, Indian Institute of Technology Roorkee, Roorkee 247 667, India (email: saikat_m@ee.iitr.ac.in; abhisek@ee.iitr.ac.in). This work was partially supported by the Science and Engineering Research Board, Department of Science and Technology, Government of India through project no: SRG/2021/001259.

In this work, an event-based sliding mode observer is proposed for estimating the states in the practical sense, i.e., the estimated states can be arbitrarily close to their actual values for any bounded disturbance. Since the classical sliding mode observer ( [19]) cannot estimate the states exactly with the external disturbance signals, a discontinuous observer was proposed in [20], [21] that ensures the exact state estimation in the presence of uncertainties. This observer injects discontinuous output error not only to reject the disturbance but also to place the observer poles. Because of this, the estimated states exhibit the undesired numerical chattering in the real-time implementation. To minimize this effect, we propose a sliding mode observer, similar to [22], that employs a discontinuous output error injection vector of the same order as that of the disturbance input. It is shown that the observer has a decoupled structure consisting of a linear part and a discontinuous part, which can be designed independently under some standard assumptions. We analyze the state estimation problem using the proposed observer in the event-triggering framework. Two popular implementation scenarios are considered. First, the actuator side implementation is considered in which the output measurements are transmitted from sensors to actuators, whereas in the second case, the sensor side estimator is developed using the output measurements directly. In both cases, the event mechanism is designed to regulate the transmission rate of plant information over the feedback channel. The practical state estimation is established by an appropriate choice of the switching gain and triggering parameter.

The layout of the paper is as follows: The problem description is given in §II. In §III, we propose a sliding mode observer with analog feedback and show the asymptotic convergence of observer states to the plant states in the presence of matched uncertainty. An event-based implementation of sliding mode observer with two popular architectures is presented in §IV. We show here the practical estimation of the proposed observers with event-based communication. All proofs of our results are collected in §V. The simulation results of the proposed observer are demonstrated in §VI. The paper is concluded with some remarks in §VII.

*Notation:* The set of real and complex numbers are symbolized by $\mathbb{R}$ and $\mathbb{C}$, respectively. The set of integers is denoted by $\mathbb{Z}$. The positive (or nonnegative) real numbers are represented as $\mathbb{R}_{>0}$ (or $\mathbb{R}_{\geqslant 0}$). Similarly, $\mathbb{Z}_{\geqslant 0}$ denotes the set of nonnegative integers. The $n$-dimensional vector space over real is given by $\mathbb{R}^n$. For a given square matrix $A \in \mathbb{R}^{n\times n}$, we write $\lambda_{\min}(A)$ and $\lambda_{\max}(A)$ to denote the minimum and maximum eigenvalues of matrix $A$, respectively. For a given vector $x \in \mathbb{R}^n$, $\|x\|$ is the Euclidean (or 2-) norm and $\|x\|_1$ is the 1-norm. The transpose of a matrix $A$ is represented as $A^\top$. The induced 2-norm of a matrix $P \in \mathbb{R}^{m\times n}$ is given by $\|P\| = \sqrt{\lambda_{\max}(P^\top P)}$. The null space of a matrix $P$ is written as $\mathcal{N}(P)$. The rank of the matrix $P$ is denoted by $\mathrm{rank}(P)$. The concatenation of two vectors $a$ and $b$ of appropriate dimensions is denoted as $\mathrm{col}(a, b)$, i.e., $\mathrm{col}(a, b) = [a^\top \ b^\top]^\top$. The cardinality of a set $S$ is given by $|S|$. We also write $|s|$ to denote the absolute value of the scalar $s$.

## II. Problem Description

Consider a continuous-time system as

$$\dot{x} = Ax + B(u + d) \tag{1a}$$
$$y = Cx \tag{1b}$$

where $x \in \mathbb{R}^n$, $u \in \mathbb{R}^m$, $d \in \mathbb{R}^m$ and $y \in \mathbb{R}^p$ represent the state vector, the control input, disturbance input and output vectors of the system, respectively. The matrices $A$, $B$, and $C$ are of appropriate dimensions and known to the designer. Here, the number of output channels is more than the inputs, i.e., $p > m$. This is essentially required to solve the robust state estimation problem in the presence of the disturbance.

*Assumption 1:* For some $d_0 > 0$, it holds that $\|d(t)\| \leqslant d_0$ for all $t \geqslant 0$.

*Assumption 2:* The column rank of the matrix $CB$ is $m$, i.e., $\operatorname{rank}(CB) = m$.

Assumption 1 is quite standard in the literature. It may be noted that the disturbance can also be a function of the state variables satisfying the bounded assumption. The second assumption states that the relative degree of the plant is one (in the multi-input multi-output sense).

The setup for addressing the estimation problem is quite different from the conventional one. Here, the output information is transmitted over the communication network at discrete instants which are not necessarily *uniformly* spaced. We adopt an event-triggering protocol for transmitting information over the network as shown in Fig. 1. A triggering condition is continuously monitored at the sensor end for generating a time sequence, and subsequently, the data are sent to the controller. Under these restrictions, we address the practical state estimation problem, which is formally defined below[1].

*Definition 1 (Practical State Estimation):* Given a dynamical system (1), the observer

$$\dot{\hat{x}} = F(\hat{x}, y, u), \qquad \hat{x}(0) \in \mathbb{R}^n$$

is said to estimate the states *practically* if for any $\varepsilon > 0$, there exists a time $T \geqslant 0$ such that $\|x(t) - \hat{x}(t)\| \leqslant \varepsilon$ for all $t \geqslant T$.

We present a sliding mode observer for solving the problem associated with the state estimation considering the event-triggering feedback. Two implementation scenarios for the observers are considered, as shown in Fig. 1. First, an actuator side implementation scheme is discussed as shown in Fig. 1(a) in which the sliding mode observer is placed at the actuator side, whereas the triggering mechanism is run at the sensor side. In the second scenario (see Fig. 1(b)), both the observer and triggering condition are located at the sensor side.

## III. Preliminary Results

This section presents a robust sliding mode observer with continuous feedback and discusses some of the key features.

### A. Coordinate Transformation

To begin with, we partition the output matrix into

$$C = \begin{bmatrix} C_1 \\ C_2 \end{bmatrix} = \begin{bmatrix} C_{11} & C_{12} \\ C_{21} & C_{22} \end{bmatrix}$$

[1]The notion of "*practical state estimation*" is borrowed from the control counterpart results on "*practical stabilization*" [23, Def. 10.1, p. 232].

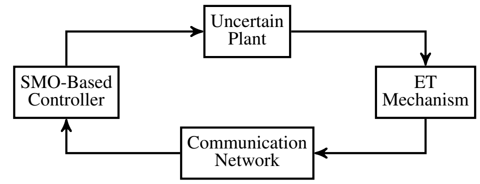


(a) Actuator side implementation

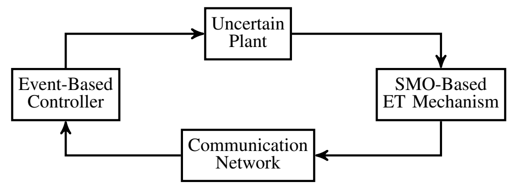


(b) Sensor side implementation

Fig. 1. Schematic depiction of event-based estimation: ET (event-triggering) and SMO (sliding mode observer).

where $C_{11} \in \mathbb{R}^{(p-m)\times(n-m)}$, $C_{12} \in \mathbb{R}^{(p-m)\times m}$, $C_{21} \in \mathbb{R}^{m\times(n-m)}$, and $C_{22} \in \mathbb{R}^{m\times m}$ represent the subblocks of $C$. Without losing generality, we assume that $C_2 B$ is an invertible matrix (hence, $C_2$ has full rank).

Let $V_1 \in \mathbb{R}^{n\times(n-m)}$ be the matrix such that its column space is $\mathcal{N}(C_2)$. Thus, $\operatorname{rank}(V_1) = n - m$. By denoting $\overline{V}_1 = (V_1^\top V_1)^{-1/2} V_1^\top$ and $\overline{C}_2 = (C_2 C_2^\top)^{-1/2} C_2$, one can verify that the matrix

$$V = \begin{bmatrix} \overline{V}_1 \\ \overline{C}_2 \end{bmatrix} \in \mathbb{R}^{n\times n}$$

is orthogonal[2]. Applying the transformation, $x \mapsto Vx =: \operatorname{col}(x_1, x_2)$, the system (1) can be transformed into

$$\begin{aligned} \dot{x}_1 &= \overline{A}_{11} x_1 + \overline{A}_{12} x_2 + \overline{B}_1 (u + d) \\ \dot{x}_2 &= \overline{A}_{21} x_1 + \overline{A}_{22} x_2 + \overline{B}_2 (u + d) \end{aligned} \tag{2}$$

where $x_1 \in \mathbb{R}^{n-m}$ and $x_2 \in \mathbb{R}^m$ are the first $n - m$ and the last $m$ elements of the modified state vector. The various matrices in (2) can be given by

$$\overline{A} = VAV^\top = \begin{bmatrix} \overline{V}_1 A \overline{V}_1^\top & \overline{V}_1 A \overline{C}_2^\top \\ \overline{C}_2 A \overline{V}_1^\top & \overline{C}_2 A \overline{C}_2^\top \end{bmatrix},$$
$$\overline{B} = VB = \begin{bmatrix} \overline{V}_1 B \\ \overline{C}_2 B \end{bmatrix} \text{ and } \overline{C} = CV^\top = \begin{bmatrix} C_1 \overline{V}_1^\top & C_1 \overline{C}_2^\top \\ 0 & C_2 \overline{C}_2^\top \end{bmatrix}$$

(we used the fact that $C_2 V_1 = 0$). Since $\overline{B}_2$ $(= \overline{C}_2 B)$ is a full rank matrix, the nonsingular transformation $z = U \operatorname{col}(x_1, x_2) = \operatorname{col}(z_1, z_2)$, where

$$U = \begin{bmatrix} I_{n-m} & -\overline{B}_1 \overline{B}_2^{-1} \\ 0 & \overline{B}_2^{-1} \end{bmatrix},$$

transforms the system (2) into

$$\dot{z}_1 = \widetilde{A}_{11} z_1 + \widetilde{A}_{12} z_2 \tag{3a}$$
$$\dot{z}_2 = \widetilde{A}_{21} z_1 + \widetilde{A}_{22} z_2 + u + d \tag{3b}$$

and the system output to

$$y = \widetilde{C} z = \begin{bmatrix} y_1 \\ y_2 \end{bmatrix} = \begin{bmatrix} \widetilde{C}_1 \\ \widetilde{C}_2 \end{bmatrix} z = \begin{bmatrix} \widetilde{C}_{11} & \widetilde{C}_{12} \\ 0 & \widetilde{C}_{22} \end{bmatrix} \begin{bmatrix} z_1 \\ z_2 \end{bmatrix}. \tag{3c}$$

[2]The orthogonal property of $V$ follows directly from $VV^\top = I_n$ and its invertibility.

The system and input matrices can be given, respectively, by

$$\widetilde{A} = \begin{bmatrix} \widetilde{A}_{11} & \widetilde{A}_{12} \\ \widetilde{A}_{21} & \widetilde{A}_{22} \end{bmatrix} \quad \text{and} \quad \widetilde{B} = \begin{bmatrix} 0 \\ I_m \end{bmatrix}.$$

The system (3a)-(3b) is already in well-known standard *regular* form with the last $m$ states being related to the plant outputs. This is required to design a sliding mode observer by injecting only $m$ number of discontinuous output errors instead of the whole vector. Indeed, these observers have additional benefits of better steady-state accuracy due to their decoupled structure ( [22]).

### B. Synthesis of Observer

We first discuss certain properties based on which the observer is to be constructed.

*Lemma 1:* If the pair $(\widetilde{A}_{11}, \widetilde{C}_{11})$ is observable, then the pair $(\widetilde{A}, \widetilde{C})$ is observable.

The above lemma guarantees the observability of the plant whenever the reduced order system (3a) is observable with respect to the first $p-m$ outputs. This essentially decouples the state reconstruction problem into two subparts, viz., a sliding mode-based discontinuous estimator and a linear observer. It may be emphasized here that a similar assumption (detectability) is used in [15] to estimate the plant state exactly with the disturbance. Here, the disturbance-free dynamics still depend on the switching component through discontinuous output error injection.

The stronger observability requirement in Lemma 1 can be avoided when

$$C_2 V_1 = C_2 A V_1 = 0 \tag{4}$$

holds, i.e., the null spaces of $C_2$ and $C_2 A$ are the same. In this case, the observability of $(\widetilde{A}_{11}, \widetilde{C}_{11})$ in Lemma 1 becomes a necessary and sufficient condition which is stated in the following corollary.

*Corollary 1:* Suppose that the equality (4) holds. Then, the pair $(\widetilde{A}, \widetilde{C})$ is observable if and only if the pair $(\widetilde{A}_{11}, \widetilde{C}_{11})$ is observable.

*Remark 1:* Corollary 1 confirms that the dynamics (3) is a cascade connection of its two subsystems (3a) and (3b). Then, the plant becomes observable if and only if each subsystem is observable with respect to their respective output. Thus, the observer synthesis for the plant is reduced to the observer synthesis for each subsystem. In other words, the estimation problem is decoupled into the same for the individual subsystem.

The sliding mode observer is synthesized as follows. From (3c), we introduce a new output function as

$$\widetilde{C}_{11} z_1 = y_1 - \widetilde{C}_{12} \widetilde{C}_{22}^{-1} y_2.$$

Then, the observer is proposed for estimating the states robustly as

$$\dot{\hat{z}}_1 = \widetilde{A}_{11} \hat{z}_1 + \widetilde{A}_{12} \hat{z}_2 + L_1 \widetilde{C}_{11}(z_1 - \hat{z}_1) + \widetilde{A}_{12}(z_2 - \hat{z}_2) \tag{5a}$$

$$\dot{\hat{z}}_2 = \widetilde{A}_{21} \hat{z}_1 + u + \widetilde{A}_{22} z_2 + K \operatorname{sign}(z_2 - \hat{z}_2) \tag{5b}$$

where $L_1 \in \mathbb{R}^{(n-m)\times(p-m)}$ is the linear observer gain, $K > 0$ is some scalar and sign function is given by $\operatorname{sign}(\gamma) = [\ \operatorname{sign}(\gamma_1) \ \ \operatorname{sign}(\gamma_2) \ \ \cdots \ \ \operatorname{sign}(\gamma_m)\ ]^\top$ for any vector $\gamma = [\ \gamma_1 \ \ \gamma_2 \ \ \cdots \ \ \gamma_m\ ]^\top$. Here, $\hat{z} = \operatorname{col}(\hat{z}_1, \hat{z}_2)$ denotes the estimate of $z = \operatorname{col}(z_1, z_2)$. It may be noted that since the observer (5) has a discontinuous right-hand side, the existence of solutions is understood in the Filippov sense ( [24]).

*Remark 2:* The observer (5) is quite similar to that proposed in [22], but it differs from it in terms of its construction. There is no additional proportional term used in (5b) unlike the case in [22]. The advantage was revealed in the analysis using a common Lyapunov function. However, in the event-triggering case (to be discussed in the latter section), the output error bound is required instead of the whole error vector and our present construction helps in realizing the same. Hence, we rely on the structure (5) and discuss its convergence analysis in detail.

*Remark 3:* The observer (5) consists of a linear part (5a) and a discontinuous subdynamics (5b). Due to this, the accuracy of the estimation process in real-time implementation is better than its existing counterparts. This is mainly because of the linear dynamics in the observer that achieve an asymptotic accuracy. Moreover, since event-triggering also involves discrete implementation, the proposed strategy has the same advantage over other classical sliding mode observers.

It can be noticed that Lemma 1 ensures the existence of the gain $L_1$ such that the eigenvalues of $\widetilde{A}_1 := \widetilde{A}_{11} - L_1 \widetilde{C}_{11}$ are stable. Then, under this assumption, we get a positive definite matrix $P_1 = P_1^\top \in \mathbb{R}^{(n-m)\times(n-m)}$ as a solution to the Lyapunov equation

$$\widetilde{A}_1^\top P_1 + P_1 \widetilde{A}_1 = -Q_1 \tag{6}$$

for any $Q_1 = Q_1^\top > 0$. With this, define the sets $\Omega_1(c_1) = \{z_1 \in \mathbb{R}^{n-m} : z_1^\top P_1 z_1 \leqslant c_1\}$ and $\Omega_2(c_2) = \{z_2 \in \mathbb{R}^m : \|z_2\| \leqslant c_2\}$ for any $c_1 > 0$ and $c_2 > 0$. Also, denote $\Omega(c_1, c_2) = \{z \in \mathbb{R}^n : z_1 \in \Omega_1(c_1) \text{ and } z_2 \in \Omega_2(c_2)\}$.

Define $\tilde{z}_1 := z_1 - \hat{z}_1$ and $\tilde{z}_2 := z_2 - \hat{z}_2$ as the estimation errors. Then, using (3) and (5), the estimation error dynamics can be expressed as

$$\dot{\tilde{z}}_1 = \widetilde{A}_1 \tilde{z}_1 \tag{7a}$$

$$\dot{\tilde{z}}_2 = \widetilde{A}_{21} \tilde{z}_1 - K \operatorname{sign}(\tilde{z}_2) + d. \tag{7b}$$

Now, the following result is immediate.

*Theorem 1:* Consider the system (3) and the observer (5). Let $c_1 > 0$ and $c_2 > 0$ be any scalars. Assume that the $(\widetilde{A}_{11}, \widetilde{C}_{11})$ pair is observable and $z(0), \hat{z}(0) \in \Omega(c_1, c_2)$. Then, there exists a gain $K > 0$ such that the estimation error $\tilde{z}(t) := z(t) - \hat{z}(t)$ is bounded for all $t \geqslant 0$, and $\tilde{z}(t) \to 0$ as $t \to +\infty$.

Note that the claims of Theorem 1 can also be shown globally under the same observability assumption. This is stated in the following corollary.

*Corollary 2:* Consider the system (3) and the observer (5). Assume that the $(\widetilde{A}_{11}, \widetilde{C}_{11})$ pair is observable. Then, there exists $K > 0$ such that the estimation error $\tilde{z}(t) := z(t) - \hat{z}(t)$ is bounded for all $t \geqslant 0$, and $\tilde{z}(t) \to 0$ as $t \to +\infty$ globally.

## IV. Event-Triggered Sliding Mode Observer

In this section, the main result of this paper is discussed. The event-triggered sliding mode observer is proposed to estimate the states of the system practically. As mentioned in §II, we discuss both the actuator and sensor side implementation cases in detail.

### A. Actuator Side Implementation

Here, the event-triggering mechanism detects a sampling instant to send the sensor output to the controller side. Let $\{t_k^y\}_{k\in\mathbb{Z}_{\geqslant 0}}$ be time instants for transmitting the output measurements. The sampled output $y(t_k^y)$ is used in the observer, and it is updated again as soon as a new measurement arrives. We propose the following event-based transmission protocol at the sensor end:

$$t_{k+1}^y = \inf\left\{t > t_k^y : \|e_y(t)\| \geqslant \sigma_a \alpha_a\right\}, \qquad k \in \mathbb{Z}_{\geqslant 0} \tag{8}$$

with $t_0^y = 0$, where

$$e_y(t) = \begin{bmatrix} \widetilde{C}_{11}\left(z_1(t_k^y) - z_1(t)\right) \\ z_2(t_k^y) - z_2(t) \end{bmatrix},$$

$\alpha_a > 0$ is the triggering (threshold) parameter, and $\sigma_a > 0$ is the attenuation factor.

With this setup, the event-based sliding mode observer is proposed as

$$\begin{aligned}\dot{\hat{z}}_1(t) &= \widetilde{A}_{11}\hat{z}_1(t) + \widetilde{A}_{12}\hat{z}_2(t) + L_1\widetilde{C}_{11}\left(z_1(t_k^y) - \hat{z}_1(t)\right)\\ &\quad + \widetilde{A}_{12}\left(z_2(t_k^y) - \hat{z}_2(t)\right)\\ \dot{\hat{z}}_2(t) &= \widetilde{A}_{21}\hat{z}_1(t) + \widetilde{A}_{22}z_2(t_k^y) + K\text{sign}\left(z_2(t_k^y) - \hat{z}_2(t)\right)\\ &\quad + u(t)\end{aligned} \tag{9}$$

for all $t \in [t_k^y, t_{k+1}^y)$ and $k \in \mathbb{Z}_{\geqslant 0}$. Note that the above observer has a similar structure to that of (5) except for the discrete output measurements. Due to this, the sampling errors are induced in the observer dynamics, which affects its steady-state accuracy. Let $e_1(t) = z_1(t_k^y) - z_1(t)$ and $e_2(t) = z_2(t_k^y) - z_2(t)$ for $t \in [t_k^y, t_{k+1}^y)$ be the sampling errors. Then, the observer dynamics (9) can be written as

$$\begin{aligned}\dot{\hat{z}}_1(t) &= \widetilde{A}_{11}\hat{z}_1(t) + \widetilde{A}_{12}\hat{z}_2(t) + L_1\widetilde{C}_{11}\tilde{z}_1(t) + \widetilde{A}_{12}\tilde{z}_2(t)\\ &\quad + L_1\widetilde{C}_{11}e_1(t) + \widetilde{A}_{12}e_2(t)\\ \dot{\hat{z}}_2(t) &= \widetilde{A}_{21}\hat{z}_1(t) + \widetilde{A}_{22}z_2(t) + K\text{sign}\left(\tilde{z}_2(t) + e_2(t)\right)\\ &\quad + u(t) + \widetilde{A}_{22}e_2(t).\end{aligned} \tag{10}$$

Using (3) and (10), the dynamics of the estimation error can be obtained as

$$\dot{\tilde{z}}_1(t) = \widetilde{A}_1\tilde{z}_1(t) - \widetilde{L}_1 e_y(t) \tag{11a}$$

$$\begin{aligned}\dot{\tilde{z}}_2(t) &= \widetilde{A}_{21}\tilde{z}_1(t) - \widetilde{A}_{22}e_2(t) - K\text{sign}\left(\tilde{z}_2(t) + e_2(t)\right)\\ &\quad + d(t)\end{aligned} \tag{11b}$$

where $\widetilde{L}_1 = \begin{bmatrix} L_1 & \widetilde{A}_{12}\end{bmatrix}$. The dynamics (11) will be useful in analyzing the convergence of estimated states.

*Theorem 2:* Consider the plant (3) and the observer (10) with the event-triggering mechanism (8). Let $\varepsilon_a > 0$ be any scalar. Suppose that the $(\widetilde{A}_{11}, \widetilde{C}_{11})$ pair is observable. Choose $c_1 > \lambda_{\min}^2(P_1)\varepsilon_a^2/(16\lambda_{\max}(P_1))$ and $c_2 > \varepsilon_a/4$. Assume that $z(0), \hat{z}(0) \in \Omega(c_1, c_2)$, and $z(t)$ is bounded for all $t \geqslant 0$. Moreover, the triggering parameter satisfies the following inequality

$$\alpha_a < \min\left\{\frac{\varepsilon_a}{2}, \sqrt{\frac{\lambda_{\min}(P_1)}{\lambda_{\max}(P_1)}}\frac{\lambda_{\min}(Q_1)}{\|P_1\widetilde{L}_1\|}\frac{\varepsilon_a}{4\sqrt{2}}\right\}. \tag{12}$$

Then, there exist $K > 0$, $\tau_a > 0$, and $T_a \geqslant 0$ such that

- the estimation error $\tilde{z}(t) := z(t) - \hat{z}(t)$ is bounded for all $t \geqslant 0$, and moreover it holds that
$$\|\tilde{z}(t)\| \leqslant \varepsilon_a, \qquad \forall\, t \geqslant T_a,$$
- $t_{k+1}^y - t_k^y \geqslant \tau_a$ for all $k \in \mathbb{Z}_{\geqslant 0}$.

The following remarks are now in order.

*Remark 4:* The assumption that the plant state, $z(t)$, is bounded for all $t \geqslant 0$ can always be fulfilled by an appropriate controller. The controller can be designed to constrain the state trajectory within some specified domain. For instance, the saturating control signal for a small time interval is a common practice followed to bound the estimation error within the desired bound, e.g., see [14]. A similar approach may also be extended to our case to fulfill these requirements.

*Remark 5:* The practical estimation is mainly achieved in our case by the triggering parameter. Due to the discrete feedback policy, the (output) sampling error enters the plant, which eventually affects the steady-state bound. Therefore, one must choose the triggering parameter appropriately to obtain an acceptable error bound. However, the smaller threshold parameter may induce a high transmission rate. This can be avoided by varying the triggering parameter online, which is quite difficult in the existing techniques.

*Remark 6:* The gain $K$ in the observer (9) depends on the additional parameters apart from those in the analog design. Here, the (additional) triggering parameter plays a crucial role in the estimation accuracy. The gain $K$ must be chosen sufficiently large to guarantee the faster convergence of estimation error and to obtain the desired steady-state bound set by the event mechanism (8). The same observations were also found in the stabilization case ( [8]).

## B. Sensor Side Implementation

The observer and triggering mechanisms are placed on the sensor side as demonstrated in Fig. 1(b). Unlike the previous case, the event mechanism uses the observer states for event detection and subsequently transmits the estimated states. Moreover, since the plant outputs can be accessed directly, the observer uses continuous output measurements to estimate the plant state.

Let $\{t_\ell^z\}_{\ell \in \mathbb{Z}_{\geqslant 0}}$ be the time sequence for transmitting the estimated values to the actuator side. The sampled value $\hat{z}(t_\ell^z)$ can be directly used in the controller for stabilizing the plant. The sliding mode observer is proposed as follows

$$\begin{aligned}\dot{\hat{z}}_1(t) &= \widetilde{A}_{11}\hat{z}_1(t) + \widetilde{A}_{12}\hat{z}_2(t) + L_1\widetilde{C}_{11}\tilde{z}_1(t) + \widetilde{A}_{12}\tilde{z}_2(t)\\ \dot{\hat{z}}_2(t) &= \widetilde{A}_{21}\hat{z}_1(t) + \widetilde{A}_{22}z_2(t) + u(t_\ell^z) + K\text{sign}\left(\tilde{z}_2(t)\right).\end{aligned} \tag{13}$$

The control signal may be transmitted from the actuator to the sensor side at the triggering instant. However, one may avoid this by computing the control law directly using the reconstructed states. In this scenario, the observer (13) can be thought of as the same structure as its analog counterpart (5). This is one of the main advantages of the sensor side implementation of the observer-based controller. Now, the event-triggering mechanism can be designed for this case as

$$t_{\ell+1}^z = \inf\left\{t > t_\ell^z : \|\hat{z}(t_\ell^z) - \hat{z}(t)\| \geqslant \sigma_s\alpha_s\right\}, \quad \ell \in \mathbb{Z}_{\geqslant 0} \tag{14}$$

with $t_0^z = 0$, where $\sigma_s > 0$ and $\alpha_s > 0$ are the design parameters. These constants are chosen as per the design requirement, like in the triggering mechanism (8).

*Theorem 3:* Consider the plant (3) and the observer (13). Let $c_1 > 0$ and $c_2 > 0$ be any scalars, and $\alpha_s > 0$ be some given constant. Suppose that the pair $(\widetilde{A}_{11}, \widetilde{C}_{11})$ is observable. Moreover, assume that $z(0), \hat{z}(0) \in \Omega(c_1, c_2)$ and $z(t)$ is bounded for all $t \geqslant 0$. Then, there exist $K > 0$ and $\tau_s > 0$ such that

- the trajectory $\tilde{z}(t)$ is bounded for all $t \geqslant 0$, and moreover $\tilde{z}(t) \to 0$ as $t \to +\infty$,
- $t_{\ell+1}^z - t_\ell^z \geqslant \tau_s$ for all $\ell \in \mathbb{Z}_{\geqslant 0}$.

*Remark 7:* As it is seen that the triggering parameter has no role in the estimation accuracy, the selection of this parameter does not depend on the observer dynamics, albeit it is an integral part of it. However, this can affect the stability of the plant dynamics through the output feedback controller. It may be observed that the triggering mechanism resembles that of the state feedback scenario, where the transmitted values are directly used in the controller. Hence, a suitable value of the triggering threshold can be chosen by considering the output feedback stabilization problem.

Since Theorem 3 guarantees the asymptotic convergence of estimation error, the estimation of state in the practical sense follows immediately. In this implementation, only sampled values of the estimated states are transmitted over the network on the occurrence of an event, and the control signal is computed using these updated values. The complete analysis with the sampling strategy (14) for the closed-loop system can be shown by considering the output feedback stabilization problem. However, this is skipped in our paper to limit the discussion only to the state estimation problem.

## V. Proofs

### A. Proof of Lemma 1

By noticing the fact that $\mathrm{rank}(\widetilde{C}_{22}) = m$, it can be observed for any $\lambda \in \mathbb{C}$ that

$$\begin{aligned}\mathrm{rank}&\left(\begin{bmatrix} \widetilde{A}-\lambda I_n \\ \widetilde{C}\end{bmatrix}\right)\\ &= \mathrm{rank}\left(\begin{bmatrix} \widetilde{A}_{11}-\lambda I_{n-m} & \widetilde{A}_{12} \\ \widetilde{A}_{21} & \widetilde{A}_{22}-\lambda I_m \\ \widetilde{C}_{11} & \widetilde{C}_{12} \\ 0 & \widetilde{C}_{22}\end{bmatrix}\right)\\ &= \mathrm{rank}\left(\begin{bmatrix} \widetilde{A}_{11}-\lambda I_{n-m} \\ \widetilde{C}_{11}\end{bmatrix}\right) + m\\ &= n\end{aligned}$$

where the last two steps follow directly from the observability of the pair $(\widetilde{A}_{11}, \widetilde{C}_{11})$. Thus, the Popov-Belevitch-Hautus (PBH) test for observability implies the result at once. ∎

### B. Proof of Corollary 1

The condition (4) implies that $\widetilde{A}_{21} = 0$ because $C_2 A V_1 = 0$. Thus, following the arguments in the proof of Lemma 1, one can conclude that the observability of $(\widetilde{A}_{11}, \widetilde{C}_{11})$ is a necessary and sufficient condition. ∎

### C. Proof of Theorem 1

To analyze the convergence of the observer states to the true state, we consider the error dynamics (7). The decoupled structure of (7) enables us to analyze their convergence property separately. Taking the Lyapunov function $V_1(\tilde{z}_1) = \tilde{z}_1^\top P_1 \tilde{z}_1$, one can show using (6) and (7a) that

$$\dot{V}_1(\tilde{z}_1) = \tilde{z}_1^\top(\widetilde{A}_1^\top P_1 + P_1\widetilde{A}_1)\tilde{z}_1 = -\tilde{z}_1^\top Q_1 \tilde{z}_1 < 0. \tag{15}$$

Since $z_1(0)$ and $\hat{z}_1(0)$ belong to $\Omega_1(c_1)$, the above inequality guarantees that the trajectory $\tilde{z}_1(t)$ never leaves the set $\Omega_1(4c_1\lambda_{\max}(P_1)/\lambda_{\min}(P_1))$ and also it converges to zero asymptotically. Hence, using this fact and Assumption 1, choose a finite gain $K$ such that

$$K > \|\widetilde{A}_{21}\|\|\tilde{z}_1(t)\| + d_0, \quad \forall\, t \geqslant 0. \tag{16}$$

By defining the Lyapunov function $V_2(\tilde{z}_2) = (1/2)\tilde{z}_2^\top \tilde{z}_2$, time derivative of $V_2(\tilde{z}_2)$ along the trajectories of (7b) shows that

$$\begin{aligned}\dot{V}_2(\tilde{z}_2) &= \tilde{z}_2^\top \dot{\tilde{z}}_2\\ &= \tilde{z}_2^\top \widetilde{A}_{21}\tilde{z}_1 - K\|\tilde{z}_2\|_1 + \tilde{z}_2^\top d\\ &\leqslant \|\widetilde{A}_{21}\|\|\tilde{z}_1\|\|\tilde{z}_2\| - K\|\tilde{z}_2\| + d_0\|\tilde{z}_2\| \end{aligned}\tag{17}$$

where we used $\|\tilde{z}_2\| \leqslant \|\tilde{z}_2\|_1$ and Assumption 1. Now, using (16), one can write the above inequality as

$$\dot{V}_2(\tilde{z}_2) \leqslant -\eta\|\tilde{z}_2\|$$

where $\eta > 0$ is some scalar. Then, it follows immediately that $\tilde{z}_2(t) \in \{\tilde{z}_2 \in \mathbb{R}^m : \|\tilde{z}_2\| \leqslant 2c_2\}$ for all $t \geqslant 0$ and $V_2(\tilde{z}_2(t)) = 0$ for all $t \geqslant 2c_2/\eta$. In other words, $z_2(t) = \hat{z}_2(t)$ for all $t \geqslant 2c_2/\eta$. This behavior of the observer (7) is often referred to as the sliding motion because the discontinuous injection term enforces $\tilde{z}_2 = 0$ in finite time. Finally, it can be claimed that $\tilde{z}(t) \in \Omega(4c_1\lambda_{\max}(P_1)/\lambda_{\min}(P_1), 2c_2)$ for all $t \geqslant 0$, and $\hat{z}(t)$ converges to the true state $z(t)$ asymptotically despite the presence of disturbance. ∎

### D. Proof of Corollary 2

This proof follows that of Theorem 1. The inequality (15) implies that for any $\tilde{z}_1(0) \in \mathbb{R}^{n-m}$, the trajectory $\tilde{z}_1(t) \to 0$ as $t \to +\infty$. Then, for any $\delta > 0$, there exists a $T_1 \geqslant 0$ such that $\|\widetilde{A}_{21}\|\|\tilde{z}_1(t)\| \leqslant \delta$ for all $t \geqslant T_1$. Let $K \geqslant \delta + d_0 + \eta$ for any scalar $\eta > 0$. Clearly, it implies the inequality (16) for all $t \geqslant T_1$. Applying the similar arguments for the subsystem (7b), we conclude that $\dot{V}_2(\tilde{z}_2(t)) \leqslant -\eta\|\tilde{z}_2(t)\|$ for all $t \geqslant T_1$. So, for any $\tilde{z}_2(0) \in \mathbb{R}^m$, one achieves $\tilde{z}_2(t) = 0$ for all $t \geqslant T_2 := T_1 + (\|\tilde{z}_2(T_1)\|/\eta)$. Therefore, the global asymptotic convergence of estimation error is guaranteed. ∎

### E. Proof of Theorem 2

At first, we write the system (3) in the compact form to simplify the analysis:

$$\dot{z} = \widetilde{A}z + \widetilde{B}(u + d) \tag{18}$$

where $\widetilde{A}$ and $\widetilde{B}$ are the compact representation of respective matrices in (3) and $z = \mathrm{col}(z_1, z_2)$ is the combined state vector.

As the event generation only depends on the plant output, we can show the existence of a uniform positive lower bound for inter-event time irrespective of the observer dynamics. For any integer $k \geqslant 0$, let $\Gamma_a = \{t \in [t_k^y, t_{k+1}^y) : \|e_y(t)\| = 0\}$. Then, for all $t \in [t_k^y, t_{k+1}^y) \setminus \Gamma_a$, one obtains

$$\frac{\mathrm{d}}{\mathrm{d}t}\|e_y(t)\| \leqslant \left\|\frac{\mathrm{d}}{\mathrm{d}t}e_y(t)\right\| = \left\|C_0\frac{\mathrm{d}}{\mathrm{d}t}z(t)\right\|$$

where $C_0 = \mathrm{diag}\{\widetilde{C}_{11}, I_m\}$. Since the plant state is bounded (by our assumption), the control input can also be bounded under the feedback law. Then, under Assumption 1, the above inequality reduces to

$$\frac{\mathrm{d}}{\mathrm{d}t}\|e_y(t)\| \leqslant \beta_a$$

for some constant $\beta_a > 0$. On solving this with $e_y(t_k^y) = 0$, one gets $\|e_y(t)\| \leqslant \beta_a(t - t_k^y)$ for $t_k^y \leqslant t < t_{k+1}^y$. Using the event condition (8), this can be written as $t_{k+1}^y - t_k^y \geqslant \tau_a := [\sigma_a\alpha_a/\beta_a]$. Further, this implies that $t_{k+1}^y - t_k^y \geqslant \tau_a$ for all $k \in \mathbb{Z}_{\geqslant 0}$, and hence we guarantee the absence of the Zeno phenomenon in the triggering mechanism.

Let us now analyze the convergence of estimation error. Taking time derivative of $V_1(\tilde{z}_1) = \tilde{z}_1^\top P_1\tilde{z}_1$ along the solution of (11a), we see that

$$\begin{aligned}\dot{V}_1(\tilde{z}_1) &= \dot{\tilde{z}}_1^\top P_1\tilde{z}_1 + \tilde{z}_1^\top P_1\dot{\tilde{z}}_1\\ &= -\tilde{z}_1^\top Q_1\tilde{z}_1 - 2\tilde{z}_1^\top P_1\widetilde{L}_1 e_y\\ &\leqslant -\lambda_{\min}(Q_1)\|\tilde{z}_1\|^2 + 2\|\tilde{z}_1\|\|P_1\widetilde{L}_1\|\|e_y\|.\end{aligned}$$

First, we see from the triggering mechanism (8) that $\|e_y(t)\| < \alpha_a$ for all $t > 0$. Then, the second term of the above inequality can be reduced using Young's inequality ( [23]) to

$$2\|\tilde{z}_1\|\|P_1\widetilde{L}_1\|\|e_y\| < \frac{\lambda_{\min}(Q_1)}{2}\|\tilde{z}_1\|^2 + 2\frac{\|P_1\widetilde{L}_1\|^2}{\lambda_{\min}(Q_1)}\alpha_a^2.$$

Applying this inequality, we can obtain

$$\dot{V}_1(\tilde{z}_1) < -\frac{\lambda_{\min}(Q_1)}{2}\|\tilde{z}_1\|^2 + 2\frac{\|P_1\widetilde{L}_1\|^2}{\lambda_{\min}(Q_1)}\alpha_a^2,$$

which further implies that

$$\dot{V}_1(\tilde{z}_1) < -\frac{\lambda_{\min}(Q_1)}{4\lambda_{\max}(P_1)}V_1(\tilde{z}_1) \qquad \forall\, V_1(\tilde{z}_1) \geqslant \theta \tag{19}$$

where $\theta := 8\alpha_a^2\lambda_{\max}(P_1)\|P_1\widetilde{L}_1\|^2/\lambda_{\min}^2(Q_1)$. Observe from (12) and $c_1 > \lambda_{\min}^2(P_1)\varepsilon_a^2/(16\lambda_{\max}(P_1))$ that $\Omega_1(\lambda_{\min}(P_1)\varepsilon_a^2/4) \subset$

$\Omega_1(4c_1\lambda_{\max}(P_1)/\lambda_{\min}(P_1))$. Thus, the inequality (19) implies that $\tilde{z}_1(t) \in \Omega_1(4c_1\lambda_{\max}(P_1)/\lambda_{\min}(P_1))$ for all $t \geqslant 0$, and moreover there exists a finite time $T_{a_1} \geqslant 0$ such that the trajectory $\tilde{z}_1(t)$ enters the set $\Omega_1(\lambda_{\min}(P_1)\varepsilon_a^2/4)$ in a time no longer than $T_{a_1}$ and remains there for all future time. Now, since $\lambda_{\min}(P_1)\|\tilde{z}_1\|^2 \leqslant V_1(\tilde{z}_1)$, one can achieve that $\|\tilde{z}_1(t)\| < \varepsilon_a/2$ for all $t \geqslant T_{a_1}$.

Let us analyze the convergence of trajectories of (11b). For the Lyapunov function $V_2(\tilde{z}_2) = (1/2)\tilde{z}_2^\top \tilde{z}_2$, it can be shown that

$$\begin{aligned}\dot{V}_2(\tilde{z}_2) &= \tilde{z}_2^\top \widetilde{A}_{21}\tilde{z}_1 - \tilde{z}_2^\top \widetilde{A}_{22}e_2 - K\tilde{z}_2^\top \operatorname{sign}(\tilde{z}_2 + e_2) + \tilde{z}_2^\top d \\ &\leqslant \|\widetilde{A}_{21}\|\|\tilde{z}_1\|\,\|\tilde{z}_2\| + \|\widetilde{A}_{22}\|\|\tilde{z}_2\|\,\|e_2\| \\ &\quad - K\tilde{z}_2^\top \operatorname{sign}(\tilde{z}_2 + e_2) + d_0\|\tilde{z}_2\| \\ &< \|\widetilde{A}_{21}\|\|\tilde{z}_1\|\,\|\tilde{z}_2\| + \alpha_a\|\widetilde{A}_{22}\|\|\tilde{z}_2\| - K\tilde{z}_2^\top \operatorname{sign}(\tilde{z}_2 + e_2) \\ &\quad + d_0\|\tilde{z}_2\|\end{aligned}$$

where we used $\|e_2\| < \alpha_a$, which follows directly from (8) and the inequality $\|e_2\| \leqslant \|e_y\|$. Further, note that (12) implies $\|e_2\| < \varepsilon_a/2$. To proceed further, we analyze the behavior of each component of $\tilde{z}_2$.

By denoting $\tilde{z}_2 = [\ \tilde{z}_{21}\ \ \tilde{z}_{22}\ \ \cdots\ \ \tilde{z}_{2m}\ ]^\top$, let $\Lambda = \{i \in \{1,2,\ldots,m\} : |\tilde{z}_{2i}| \leqslant \varepsilon_a/(2\sqrt{m})\}$, i.e., the set of indices of components of $\tilde{z}_2$ that lie within their respective sets $\{\tilde{z}_{2i} : |\tilde{z}_{2i}| \leqslant \varepsilon_a/(2\sqrt{m})\}$. Also, denote $\overline{\Lambda} = \{1,2,\ldots,m\} \setminus \Lambda$. Then, we denote by $\tilde{z}_{2\Lambda}$ ($\tilde{z}_{2\overline{\Lambda}}$) the vector consisting of components of $\tilde{z}_2$ whose indices belong to the set $\Lambda$ ($\overline{\Lambda}$). With this, consider the case $\Lambda = \emptyset$. Here, none of the components of $\tilde{z}_2$ crosses the set $\{\tilde{z}_{2i} : \tilde{z}_{2i} = 0\}$. Thus, one achieves that $\operatorname{sign}(\tilde{z}_2 + e_2) = \operatorname{sign}(\tilde{z}_2)$ and this leads to

$$\dot{V}_2(\tilde{z}_2) < \|\widetilde{A}_{21}\|\|\tilde{z}_1\|\,\|\tilde{z}_2\| + \alpha_a\|\widetilde{A}_{22}\|\|\tilde{z}_2\| - K\|\tilde{z}_2\| + d_0\|\tilde{z}_2\|.$$

Since $\tilde{z}_1(t)$ is bounded for all $t \geqslant 0$, we can select a switching gain satisfying

$$K \geqslant \|\widetilde{A}_{21}\|\|\tilde{z}_1(t)\| + \alpha_a\|\widetilde{A}_{22}\| + d_0 + \eta \tag{20}$$

for all $t \geqslant 0$ and any $\eta > 0$, and eventually obtain that

$$\dot{V}_2(\tilde{z}_2) < -\eta\|\tilde{z}_2\|. \tag{21}$$

Using the fact that $c_2 > \varepsilon_a/4$, one may note $\Omega_2(\varepsilon_a/2) \subset \Omega_2(2c_2)$. Therefore, the inequality (21) guarantees that the trajectory $\tilde{z}_2$ starting from $\Omega_2(2c_2)$ enters the set $\Omega_2(\varepsilon_a/2)$ in a finite time. Now, for the case $\Lambda \neq \emptyset$, one can write

$$\dot{\tilde{z}}_{2\overline{\Lambda}} = \widetilde{A}_{21_{\overline{\Lambda}}}\tilde{z}_1 - \widetilde{A}_{22_{\overline{\Lambda}}}e_2 - K\operatorname{sign}\left(\tilde{z}_{2\overline{\Lambda}} + e_{2\overline{\Lambda}}\right) + d_{\overline{\Lambda}}$$

where $\widetilde{A}_{21_{\overline{\Lambda}}}$ and $\widetilde{A}_{22_{\overline{\Lambda}}}$ are the matrices $\widetilde{A}_{21}$ and $\widetilde{A}_{22}$, respectively, corresponding to the row indices in $\overline{\Lambda}$. Again, since none of the components of $\tilde{z}_{2\overline{\Lambda}}$ cross the set $\{\tilde{z}_{2\overline{\Lambda}} : \tilde{z}_{2\overline{\Lambda}} = 0\}$, we have $\operatorname{sign}\left(\tilde{z}_{2\overline{\Lambda}} + e_{2\overline{\Lambda}}\right) = \operatorname{sign}\left(\tilde{z}_{2\overline{\Lambda}}\right)$. Then, applying these facts together with (20), one can show that

$$\begin{aligned}\dot{V}_2(\tilde{z}_{2\overline{\Lambda}}) &< \left\|\widetilde{A}_{21_{\overline{\Lambda}}}\right\|\|\tilde{z}_1\|\ \left\|\tilde{z}_{2\overline{\Lambda}}\right\| + \alpha_a\left\|\widetilde{A}_{22_{\overline{\Lambda}}}\right\|\left\|\tilde{z}_{2\overline{\Lambda}}\right\| - K\left\|\tilde{z}_{2\overline{\Lambda}}\right\| \\ &\quad + d_0\|\tilde{z}_{2\overline{\Lambda}}\| \\ &\leqslant -\eta\left\|\tilde{z}_{2\overline{\Lambda}}\right\|.\end{aligned} \tag{22}$$

This shows that the trajectory $\tilde{z}_{2\overline{\Lambda}}$ converges towards the set $\{\tilde{z}_{2\overline{\Lambda}} : \|\tilde{z}_{2\overline{\Lambda}}\| \leqslant \varepsilon_a/2\}$ in a finite time. Moreover, if a component of $\tilde{z}_2$ enters the set $\{\tilde{z}_{2i} : |\tilde{z}_{2i}| \leqslant \varepsilon_a/(2\sqrt{m})\}$, it cannot leave this set due to (22). Thus, from the inequalities (21) and (22), it can be concluded that the trajectory $\tilde{z}_2$ enters the set $\Omega_2(\varepsilon_a/2)$ in a finite time, say $T_{a_2} \geqslant 0$ and remains there for all future time. Therefore, $\tilde{z}(t)$ remains bounded within the set $\Omega(4c_1\lambda_{\max}(P_1)/\lambda_{\min}(P_1), 2c_2)$ for all $t \geqslant 0$ and moreover $\tilde{z}(t) \in \Omega(\lambda_{\min}(P_1)\varepsilon_a^2/4, \varepsilon_a/2)$ for all $t \geqslant T_a := \max\{T_{a_1}, T_{a_2}\}$. Finally, we obtain

$$\|\tilde{z}(t)\| \leqslant \|\tilde{z}_1(t)\| + \|\tilde{z}_2(t)\| < \frac{\varepsilon_a}{2} + \frac{\varepsilon_a}{2} = \varepsilon_a$$

for all $t \geqslant T_a$. This completes the proof. ■

### F. Proof of Theorem 3

Let $\tau > 0$ be the maximum time such that the trajectory $\hat{z}(t)$ is bounded on the interval $[0, \tau]$. One may write the error dynamics using (3) and (13) as

$$\begin{aligned}\dot{\tilde{z}}_1 &= \widetilde{A}_1\tilde{z}_1 \\ \dot{\tilde{z}}_2 &= \widetilde{A}_{21}\tilde{z}_1 - K\operatorname{sign}(\tilde{z}_2) + d\end{aligned}$$

which is the same as (7). Following the arguments of Theorem 1, we can claim that the error trajectory $\tilde{z}(t)$ is also bounded on the interval $[0, \tau]$. Since both the estimated states and error trajectories are bounded on the interval $[0, \tau]$, there exists a constant $\beta_s > 0$ such that $(\mathrm{d}/\mathrm{d}t)\|\hat{z}(t)\| \leqslant \beta_s$ for all $t \in [0, \tau]$. Let $\Gamma_s = \{t \in [t_\ell^z, t_{\ell+1}^z) : \|e_z(t)\| = 0\}$, where $e_z(t) = \hat{z}(t_\ell^z) - \hat{z}(t)$. Then, for any integer $\ell \geqslant 0$ such that $([t_\ell^z, t_{\ell+1}^z) \setminus \Gamma_s) \subset [0, \tau]$, solving the differential inequality

$$\frac{\mathrm{d}}{\mathrm{d}t}\|e_z(t)\| \leqslant \beta_s$$

with $\|e_z(t_\ell^z)\| = 0$ yields that $\|e_z(t)\| \leqslant \beta_s(t - t_\ell^z)$ for all $t \in [t_\ell^z, t_{\ell+1}^z)$. Using (14), one gets $t_{\ell+1}^z - t_\ell^z \geqslant \tau_s := [\sigma_s\alpha_s/\beta_s]$, which confirms no Zeno phenomenon on the interval $[0, \tau]$. Now, since the plant state is bounded (by our assumption) and error trajectory has asymptotic convergence property, one can conclude from $\|\hat{z}(t)\| \leqslant \|z(t)\| + \|\tilde{z}(t)\|$ for each $t \geqslant 0$ that the estimated trajectory is also bounded for all time. Thus, $\tau = +\infty$, i.e., $\hat{z}(t)$ is bounded for all $t \geqslant 0$, and the above arguments hold for all time. This completes the proof. ■

## VI. Simulation Results

A linearized model of the inverted pendulum ([25]) is considered here to demonstrate the proposed approach. The plant is given by

$$A = \begin{bmatrix} 0 & 0 & 1 & 0 \\ 0 & 0 & 0 & 1 \\ 0 & -1.9333 & -1.9872 & 0.0091 \\ 0 & 36.9771 & 6.2589 & -0.1738 \end{bmatrix},\ B = \begin{bmatrix} 0 \\ 0 \\ 0.3205 \\ -1.0095 \end{bmatrix}$$

and $C = [\ I_3\ \ 0\ ]$. The state vector $x = [\ x_p\ \ \theta\ \ \dot{x}_p\ \ \dot{\theta}\ ]^\top$ represents componentwise the cart position, the angular position of the pendulum from the vertical axis, and their velocities, respectively. Now, applying the following transformations sequentially on the above plant

$$V = \begin{bmatrix} 0 & 1 & 0 & 0 \\ -1 & 0 & 0 & 0 \\ 0 & 0 & 0 & 1 \\ 0 & 0 & 1 & 0 \end{bmatrix} \text{ and } U = \begin{bmatrix} 1 & 0 & 0 & 0 \\ 0 & 1 & 0 & 0 \\ 0 & 0 & 1 & 3.1497 \\ 0 & 0 & 0 & 3.1201 \end{bmatrix},$$

one obtains the system dynamics in the new coordinate $z = UVx$ with

$$\widetilde{A}_{11} = \begin{bmatrix} 0 & 0 & 1 \\ 0 & 0 & 0 \\ 30.8878 & 0 & -0.1451 \end{bmatrix} \text{ and } \widetilde{C}_{11} = \begin{bmatrix} 0 & -1 & 0 \\ 1 & 0 & 0 \end{bmatrix}.$$

We verify that $(\widetilde{A}_{11}, \widetilde{C}_{11})$ pair is observable. Then, we obtain the linear observer gain $L_1 = \begin{bmatrix} 0 & 2.0349 \\ -1.79 & 0 \\ 0 & 31.7694 \end{bmatrix}$ which places the

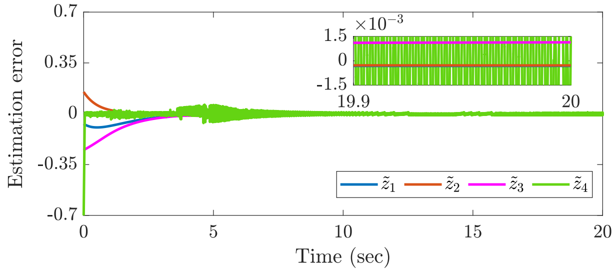


(a) Error trajectories with time.

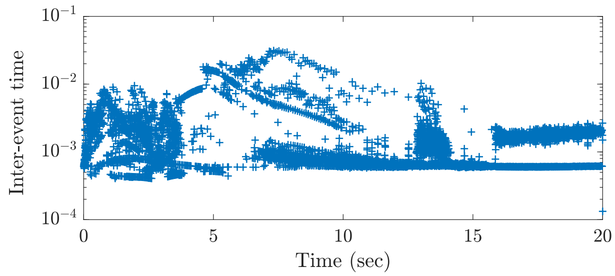


(b) Inter-event time versus time.

Fig. 2. Actuator side implementation of the event-triggered observer.

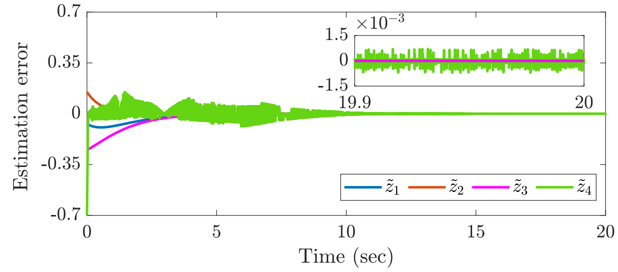


(a) Error trajectories with time.

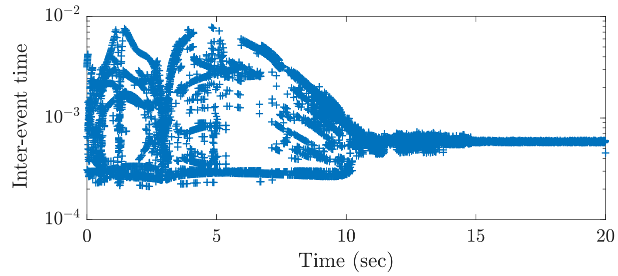


(b) Inter-event time versus time.

Fig. 3. Sensor side implementation of the event-triggered observer.

eigenvalues of $\widetilde{A}_1$ at $-1.2$, $-0.98$ and $-1.79$. On solving (6) with $Q_1 = I_3$, one gets $P_1 = \begin{bmatrix} 0.4285 & 0 & -0.3719 \\ 0 & 0.2793 & 0 \\ -0.3719 & 0 & 1.1882 \end{bmatrix}$. The disturbance signal is $d(t) = 0.2\sin t$ in our simulation study.

*Actuator Side Implementation:* We choose $\varepsilon_a = 5.0469$ to meet our design criteria. Then, we fix $c_1 = 0.0967$ and $c_2 = 2$ so that the design constraints, i.e., $c_1 > 0.0910$ and $c_2 > 1.2617$, are met. The triggering parameter is taken as $\alpha_a = 0.0099$ satisfying (12). Also, $\sigma_a = 0.98$. It can be verified that $z(0) = \begin{bmatrix} 0.07 & -0.15 & 0.25 & 0.7 \end{bmatrix}^\top$ and $\hat{z}(0) = \begin{bmatrix} 0 & 0 & 0 & 0 \end{bmatrix}^\top$ belong to the set $\Omega(c_1, c_2)$. The observer switching gain $K$ that satisfies (20) is found to be 16. Now, the simulation is run for 20 seconds, and then, the corresponding results are presented in Fig. 2. Here, we see that the estimation errors are bounded within finite time as given in Theorem 2 (see Fig. 2(a)). The numerical chattering in the estimation error is observed due to the large observer switching gain. It is also possible to reduce the switching gain without violating the stability requirement that can achieve better steady-state accuracy. The effect of large switching gain is observed in the inter-event time as depicted in Fig. 2(b). With larger switching gain, the inter-event times are decreased, although a uniform positive lower bound is guaranteed. Therefore, no Zeno behavior is exhibited in the triggering sequence. During the inter-event time period, the communication channel is left free, and it can be utilized for accomplishing other parallel tasks. It should be noted that the estimation error bound can be reduced by modifying the triggering threshold, but it may increase computational and communication burdens. So, a trade-off value of the triggering parameter can be chosen depending on the requirement. Moreover, one can tune it online without affecting the stability of the closed-loop system.

*Sensor Side Implementation:* In this case, we consider the same initial conditions for $\hat{z}(0)$ and $z(0)$. Thus, $z(0), \hat{z}(0) \in \Omega(c_1, c_2)$. Also, the switching gain $K$ and the triggering parameters are kept unchanged. Then, we run the simulation for the same duration, and the results are shown in Fig. 3. From Fig. 3(a), we observe that the estimation error converges to zero asymptotically with some numerical chattering. Like in the actuator side implementation, this is attributed to the very large switching gain used in the observer. However, in the real-time scenario, the gain can be varied in a manner that stability is guaranteed and a desired accuracy is met. In Fig. 3(b), it is seen that the sampling periods are non-zero, implying no accumulation of triggering instants. It may be highlighted that a larger lower bound can be obtained by decreasing the switching gain.

## VII. Conclusion

We proposed an event-based sliding mode observer for estimating the states practically, i.e., with any arbitrary accuracy. It was possible by the proper tuning of event parameters, possibly online. We discussed the implementation of the observer in two different architectures. In the first one, we proved that the states are estimated practically irrespective of external disturbances. However, in sensor-side implementation, the estimation error converges to zero as the outputs are continuously fed to the observer. The proposed sliding mode observer can be useful for various applications, e.g., fault detection and isolation, output feedback stabilization, detection of cyber-attacks, etc.

## References

[1] B. Sinopoli, L. Schenato, M. Franceschetti, K. Poolla, M. I. Jordan, and S. S. Sastry, "Kalman filtering with intermittent observations," *IEEE Trans. Autom. Control*, vol. 49, no. 9, pp. 1453–1464, 2004.

[2] H. K. Khalil and L. Praly, "High-gain observers in nonlinear feedback control," *Int. J. Robust and Nonlinear Control*, vol. 24, no. 6, pp. 993–1015, 2014.

[3] W. P. Heemels, K. H. Johansson, and P. Tabuada, "An introduction to event-triggered and self-triggered control," in *Proc. 51st IEEE Conf. Decis. Control*. IEEE, 2012, pp. 3270–3285.

[4] K. J. Åström and B. M. Bernhardsson, "Comparison of Riemann and Lebesgue sampling for first order stochastic systems," in *Proc. 41st IEEE Conf. Decis. Control*, vol. 2. IEEE, 2002, pp. 2011–2016.

[5] P. Tabuada, "Event-triggered real-time scheduling of stabilizing control tasks," *IEEE Trans. Autom. Control*, vol. 52, no. 9, pp. 1680–1685, 2007.

[6] X. Yi, K. Liu, D. V. Dimarogonas, and K. H. Johansson, "Dynamic event-triggered and self-triggered control for multi-agent systems," *IEEE Trans. Autom. Control*, vol. 64, no. 8, pp. 3300–3307, 2018.

[7] B. Bandyopadhyay and A. K. Behera, *Event-Triggered Sliding Mode Control*. Springer, 2018, vol. 139.

[8] A. K. Behera, B. Bandyopadhyay, and X. Yu, "Periodic event-triggered sliding mode control," *Automatica*, vol. 96, pp. 61–72, 2018.

[9] A. K. Behera, B. Bandyopadhyay, M. Cucuzzella, A. Ferrara, and X. Yu, "A survey on event-triggered sliding mode control," *IEEE J. Emerging and Selected Topics Ind. Electronics*, vol. 2, no. 3, pp. 206–217, 2021.

[10] Y. Huang, J. Wang, D. Shi, and L. Shi, "Toward event-triggered extended state observer," *IEEE Trans. Autom. Control*, vol. 63, no. 6, pp. 1842–1849, 2017.

[11] X. Meng and T. Chen, "Optimal sampling and performance comparison of periodic and event based impulse control," *IEEE Trans. Autom. Control*, vol. 57, no. 12, pp. 3252–3259, 2012.

[12] J. Huang, D. Shi, and T. Chen, "Robust event-triggered state estimation: A risk-sensitive approach," *Automatica*, vol. 99, pp. 253–265, 2019.

[13] P. Tallapragada and N. Chopra, "Event-triggered dynamic output feedback control for LTI systems," in *Proc. 51st IEEE Conf. Decis. Control*. IEEE, 2012, pp. 6597–6602.

[14] A. K. Behera and H. Shim, "Robust feedback stabilization using high-gain observer via event triggering," *Int. J. Robust and Nonlinear Control*, vol. 30, no. 5, pp. 2097–2112, 2020.

[15] C. Edwards and S. K. Spurgeon, *Sliding Mode Control: Theory and Applications*. CRC Press, 1998.

[16] W. Cai, J. She, M. Wu, and Y. Ohyama, "Disturbance suppression for quadrotor UAV using sliding-mode-observer-based equivalent-input-disturbance approach," *ISA Trans.*, vol. 92, pp. 286–297, 2019.

[17] F. Han, L. Xu, X. Yu, Z. Tari, Y. Feng, and J. Hu, "Sliding-mode observers for real-time DDoS detection," in *Proc. 11th IEEE Conf. Ind. Electronics and Appl.* IEEE, 2016, pp. 825–830.

[18] H. Amara, S. Latreche, M. Sid, and M. Khemliche, "Sliding mode observer and event triggering mechanism co-design," *Engineering, Technology & Applied Science Research*, vol. 10, no. 2, pp. 5487–5491, 2020.

[19] S. Drakunov and V. Utkin, "Sliding mode observers: Tutorial," in *Proc. 34th IEEE Conf. Decis. Control*, vol. 4. IEEE, 1995, pp. 3376–3378.

[20] C. Edwards and S. K. Spurgeon, "On the development of discontinuous observers," *Int. J. Control*, vol. 59, no. 5, pp. 1211–1229, 1994.

[21] S. K. Spurgeon, "Sliding mode observers: a survey," *Int. J. Systems Science*, vol. 39, no. 8, pp. 751–764, 2008.

[22] A. K. Behera, S. Mondal, and B. Bandyopadhyay, "A decoupled design of a robust sliding mode observer," *Automatica*, vol. 148, p. 110799, 2023.

[23] H. K. Khalil, *Nonlinear Control*. Pearson New York, 2015, vol. 406.

[24] A. F. Filippov, *Differential Equations With Discontinuous Righthand Sides*. Kluwer Academic Publishers, Dordrecht, The Netherlands, 1988.

[25] C. Edwards, S. K. Spurgeon, and R. J. Patton, "Sliding mode observers for fault detection and isolation," *Automatica*, vol. 36, no. 4, pp. 541–553, 2000.